

Guided Sampling-based Evolutionary Deep Neural Network for Intelligent Fault Diagnosis

Arun K. Sharma, *Student Member, IEEE* and Nishchal K. Verma, *Senior Member, IEEE*

Abstract—The diagnostic performance of most of the deep learning models is greatly affected by the selection of model architecture and their hyperparameters. The main challenges in model selection methodologies are the design of architecture optimizer and model evaluation strategy. In this paper, we have proposed a novel framework of evolutionary deep neural network which uses policy gradient to guide the evolution of DNN architecture towards maximum diagnostic accuracy. We have formulated a policy gradient-based controller which generates an action to sample the new model architecture at every generation. The best fitness obtained is used as a reward to update the policy parameters. Also, the best model obtained is transferred to the next generation for quick model evaluation in the NSGA-II evolutionary framework. Thus, the algorithm gets the benefits of fast non-dominated sorting as well as quick model evaluation. The effectiveness of the proposed framework has been validated on three datasets: the Air Compressor dataset, Case Western Reserve University dataset, and Paderborn university dataset.

Impact Statement—Nowadays even if there are a lot of advancements in computational intelligence, intelligent fault diagnosis requires good expertise to design the diagnostic model. This is because the performance of most of the diagnostic models depends on model selection and hyperparameters. The proposed method of guided sampling-based evolutionary deep neural network non-dominated sorting-based evolutionary algorithm to optimize the model architecture. The model architecture is sampled by using a reward-based policy to force the evolutionary algorithm to get a model architecture that can give maximum accuracy. Therefore, the proposed method is the best solution for the model architecture selection without any human expertise while ensuring the best possible diagnostic performance.

Index Terms—Neural architecture search, Intelligent fault diagnosis, Deep neural network, Non-dominated sorting algorithm, Policy gradient.

I. INTRODUCTION

WITH the advancement in modern computational technology, machine learning based intelligent fault diagnosis has become an integral part of almost all industrial sectors. Intelligent fault diagnosis refers to the preventive maintenance of industrial machines using machine learning-based data analysis and class detection [1]–[6]. Data-driven fault diagnosis of industrial machines faces many challenges: (i) labeled data availability as running the machine in a faulty state with real-time load is not possible, (ii) training the deep learning algorithms with limited availability of labeled dataset, (iii) model selection best suited for the dataset under consideration. A deep neural network (DNN) has been commonly used for intelligent fault diagnosis due to its high capability of non-linear feature transformation [7], [8]. However, training the

DNN from scratch for every change in the operating condition of the machine becomes an uneconomical process. To solve such problems, many researchers have suggested a variety of domain adaptation methods [9]–[16]. [11], [14] and [15] uses labeled source dataset from the laboratory machine and the unlabeled target dataset from the test machine to train a model capable to diagnose the fault on the test dataset from the target machine. A quick learning mechanism to train the model in the target domain by transforming an already trained model on source data. All these methods work well only if a suitable architecture is selected based on trial and error and some prior experience with the dataset. In practice, it becomes a big challenge for selecting and training the best suitable architecture with every change in the dataset due to variations in machine operating conditions and fault types.

Therefore, our main objective is to investigate and develop an algorithm that can find a best suitable architecture for the given dataset with limited computational resources and computational time. As the performance of most of the deep learning algorithms is very much affected by the hyper-parameters, research on hyper-parameter optimization or neural architecture search (NAS) has gained very much attention nowadays [17], [18]. Based on architecture optimization strategy, NAS methods are mainly categorized as: (i) random search and grid search [19], (ii) surrogate model-based optimization [20], (iii) reinforcement learning [21], (iv) genetic algorithm [22]–[26], (v) gradient descent [27], and (vi) hybrid algorithms [28]. In most of the aforementioned methods, the biggest challenge for architecture search is the model evaluation because of the complex training mechanism for most of the deep learning models [18]. In genetic algorithm-based NAS methods, the evolution of architecture takes many days of GPU. For example, regularized evolution of image classifier [29] with 450 K40 GPU takes 3150 GPU days. Architecture optimization using non-dominated sorting genetic algorithm II (NSGA-II [30]) has also gained much attention due to the fast sorting framework [26], [31]. EvoN2N [26] uses the concept of knowledge transfer for fitness evaluation in the NSGA-II based framework. The quick fitness evaluation with fast NSGA-II makes the algorithm faster compared to the state-of-the-art evolutionary methods. In this paper, we extend the work of EvoN2N [26] to introduce a guided sampling-based evolution that makes the convergence faster while exploiting the search space with the help of a reward-based controller. The key contributions of this work are highlighted below

- i) We have formulated the guided sampling-based evolution of DNN architecture (**GS-EvoDNN**) using policy gradient.

Arun K. Sharma and Nishchal K. Verma are with the Dept. of Electrical Engineering, Indian Institute of Technology, Kanpur, India. e-mail: arnks@iitk.ac.in and nishchal@iitk.ac.in

- ii) We have introduced a mean and variance term to exploit the search space for the model optimization.
- iii) We have formulated an update law for mean and variance term using policy gradient.
- iv) We have adopted the knowledge transfer mechanism to initialize the weight matrices of the model at a generation by using the best model from the previous generation.

The rest of the article is organized as follows. Table I summarizes the symbols commonly used throughout the literature except index variables on summation and loop variables in algorithmic steps. Section II defines the objective problem. Section III briefly discusses the related works and the theoretical backgrounds. Section IV explains the implementation details of the proposed framework of GS-EvoDNN. Section V discussed the effectiveness of the proposed framework for fault diagnosis under various load and operating conditions of the machine. And finally, Section VI concludes the whole paper.

Table I: LIST OF SYMBOLS

Symbol	Description
$\mathcal{D}^{tr}, \mathcal{D}^{val}, \& \mathcal{D}^{te}$	Dataset, training, validation & test dataset
$\mathbf{X} \in \mathbb{R}^{(n_s \times n_f)}, \mathbf{y} \in \mathbb{R}^{n_s}$	Input data, Output labels
$n_s \& n_f$	Number of samples & features
C	number class of the dataset
Ψ_t	DNN model at generation t
Ψ_t^\dagger	Best DNN model at generation t
Λ_t, \mathcal{R}_t	Fitness matrix, Rank at generation t
P_t, Q_t	Population, Offspring at generation t
n_p	number hidden layers in p^{th} model
h_k	Number nodes in k^{th} hidden layer

II. PROBLEM STATEMENT

Let the training dataset, validation dataset, and test dataset are $\mathcal{D}^{tr} = (\mathbf{X}^{tr}, \mathbf{y}^{tr})$, $\mathcal{D}^{val} = (\mathbf{X}^{val}, \mathbf{y}^{val})$, and $\mathcal{D}^{te} = (\mathbf{X}^{te}, \mathbf{y}^{te})$, respectively where $\mathbf{X} \in \mathbb{R}^{(n_s \times n_f)}$ be the input data with n_s samples & n_f features and $\mathbf{y} \in \mathbb{R}^{n_s}$ be the corresponding output label. The objective of optimal DNN architecture search for fault classification is mathematically be formulated as

$$\Psi^\dagger = \mathcal{H}(P, \mathcal{D}^{tr}, \mathcal{D}^{val}) \quad (1)$$

$$\hat{\mathbf{y}}^{te} = \mathcal{F}(\Psi^\dagger, \mathbf{X}^{te}) \quad (2)$$

where $\mathcal{H}(\cdot)$ denotes the optimization function to get the best model Ψ^\dagger with optimal parameters for the training dataset and $\mathcal{F}(\cdot)$ is the feed-forward DNN function which predicts the fault class $\hat{\mathbf{y}}^{te}$ for the test data \mathbf{X}^{te} .

III. RELATED WORKS AND THEORETICAL BACKGROUND

A. Deep Neural Network (DNN)

The deep neural network (DNN): a multi-layered neural network is the most popular technique for pattern recognition via non-linear feature transformation in multiple stages [32]. From the training point of view, DNN can be considered as two parts: Stack of a given number of auto-encoders (also called stacked auto-encoder: SAE) [33] and a classifier

usually softmax classifier as output layer. First, a greedy layer unsupervised training is used to train each of the auto-encoder (AE) in the SAE. Then, the SAE stacked with the classifier at the end layer is fine-tuned using a labeled training dataset. The SAE with softmax classifier (DNN model Ψ) is depicted in Fig. 1.

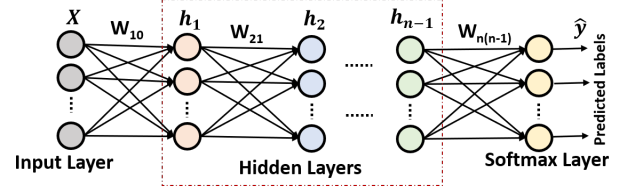


Fig. 1: SAE with softmax classifier (DNN model: Ψ)

B. Intelligent Fault Diagnosis

Recently, with the advent of advanced machine learning techniques and the availability of fast computational resources, the data-driven intelligent fault diagnosis method has gained much popularity, [1]–[4]. In these methods, various machine learning techniques are utilized to learn the specific signature of the recorded signals like current, vibration, temperature, etc., and thereafter identify the existence of machinery fault using the test samples. Neural network (NN) [34], Support vector machine (SVM) [35], [36], and random forest (RF) classifier [5] have been very effectively used for intelligent fault diagnosis and have been proved to be the baseline method for pattern recognition. But the diagnostic performances by these methods are reduced due to high sparsity and low-quality features in the dataset [37]. The intelligent fault diagnosis using deep learning methods has gained much attention due to its capability of multi-scale hierarchical feature transformation and large dimensional data handling, [7], [8], [14]. However, using a deep neural network for fault diagnosis faces a major challenge of training from scratch for every new operating condition of the machines. The recent trend of using deep transfer learning methods for domain adaptation has been very effective for fault diagnosis under changeable operating conditions [9], [10], [12], [13], [15], [16], [38]. However, the diagnosis performance by these methods is very much affected by the selection of the architecture of the deep neural network and the other hyper-parameters.

C. Neural Architecture Search (NAS)

The main objective of NAS methods is to obtain the optimal architecture in a given search space with the best model performance [18]. There are three important aspects of the NAS methods: (i) formulation of the search space, (ii) the architecture optimizer, and (iii) the model evaluation. Formulation of search space defines the design format for the model architecture. It can be categorized into four groups: (i) cell-based (ii) entire-structured, (iii) morphism-based, and (iv) hierarchical search space. The most important aspect of NAS methods is the model evaluation as it is computationally very expensive to train each model during the search process and

evaluate on the unseen dataset. To accelerate the evolution, various mechanism have been suggested for the model evaluation [18], [20], [29], [39]–[43]. K. Kandasamy, *et.al.*, [41] suggested learning the curve extrapolation for the model performance evaluation instead to train and evaluate the actual architecture. H. Pham *et. al.*, [43] proposed the method of parameter sharing for the faster training and evaluation of the model architecture.

Another important aspect of NAS methods is the architecture optimizer (AO). The objective automatic AO is to automatically guide the model architecture search in a direction to get the best suitable model for a given dataset. The AO methods adopted by various researchers can be categorized as (i) random search (RS) (ii) grid search (GS), (iii) surrogate model-based optimization (SMBO), (iv) gradient descent (GD), (v) reinforcement learning (RL), (vi) genetic algorithms (GA), and (vii) hybrid methods. In the RS method, the search optimizer tries different architecture randomly from the defined search space, [19], whereas, in GS, the search method uses a grid to sample and evaluate the model architecture [40]. SMBO methods use Basian optimization [20], [41], [42] or neural networks [44] as a surrogate model of the objective function to obtain the most promising solution (the model architecture). Gradient descent-based method uses softmax function to find the optimal architecture over a continuous and differentiable search space [27]. In RL-based NAS [21], [45], a controller (usually, a recurrent neural network) generate an action to sample a new architecture. The observation (state) & the reward from the environment is used to update the controller policy to generate new architecture samples. Here, the training & validation process of the sampled neural network is treated as the environment that returns back the validation accuracy. GA-based NAS [22]–[25], [31], [46], use heuristic search to find the best performing architecture over a given search space. In these methods, heuristically sampled neural architectures are trained and evaluated using the convention neural training methods and the performance metrics are used as fitness for evolution to obtain the optimal architecture. The main challenge of these methods is the fitness evaluation of the individual model. All of these methods of AO have their own merits and demerits. The hybridization of two of the above methods may give a significant improvement in the search efficiency, called the hybrid method of AO [28], [47], [48].

D. Policy Gradient

Policy gradient (PG) is a tool to optimize the controller policy for reinforcement learning algorithm [49], [50]. The controller policy is the parameterized function that defines the learning agent's way to act on the environment to get maximum reward Fig. 2. The reward defines the good or bad effect of the action taken by the policy towards the fulfillment of the optimal objective. Let the parameter vector be θ_t , then the parameterized function policy is represented as $\pi_{\theta_t}(a_t|s_t)$, where a_t and s_t represent action and state at given time t . Let the action a_t produces reward r_{t+1} from the environment, then the trajectory of state, action and reward can be represented as $((s_0, a_0, r_1), (s_1, a_1, r_2), \dots, (s_t, a_t, r_{t+1}))$. The policy parameter θ_t can be updated using policy gradient

as

$$\theta_{t+1} = \theta_t + \eta_t \nabla_{\theta_t} \mathcal{J}(\theta_t) \quad (3)$$

where η_t denotes the learning rate at time t , usually a constant real number. $\nabla_{\theta_t} \mathcal{J}(\theta_t)$ denotes the policy gradient and can be calculated using expected of cumulative reward U_t over the time t as follows.

$$\nabla_{\theta_t} \mathcal{J}(\theta_t) = \nabla_{\theta_t} E[U_t] = \nabla_{\theta_t} \int \pi(\tau) r(\tau) d(\tau) \quad (4)$$

$$= E[r(\tau) \cdot \nabla_{\theta_t} \log \pi_{\theta_t}(\tau)] \quad (5)$$

$$\nabla_{\theta_t} \mathcal{J}(\theta_t) = \frac{1}{N} \sum_{k=1}^N r(k) \left(\sum_{t=1}^T \nabla_{\theta_t} \log \pi_{\theta_t}(a_t | a_{t-1:1}; \theta_t) \right) \quad (6)$$

IV. PROPOSED FRAMEWORK

In this section, the proposed framework of guided sampling-based evolutionary DNN (GS-EvoDNN) is described in detail. The Fig 2 shows the schematic of the workflow of GS-EvoDNN. In the figure, DNN architecture optimization in the NSGA-II framework constitute the environment. The fitness of the best model is termed as the reward. The sorted fitness of all the individuals in the population is treated as the state of the controller. The controller policy π_{θ_t} generates an action $a_t = [m_t, \sigma_t]$, where m_t and σ_t be the mean and variance for the sampling of DNN architecture at generation t . Given the training dataset \mathcal{D}^{tr} and the validation dataset \mathcal{D}^{val} , the algorithmic steps for the GS-EvoDNN is presented in Algorithm 1. Our contributions are highlighted in Algorithm 1 and are further discussed in the following sections.

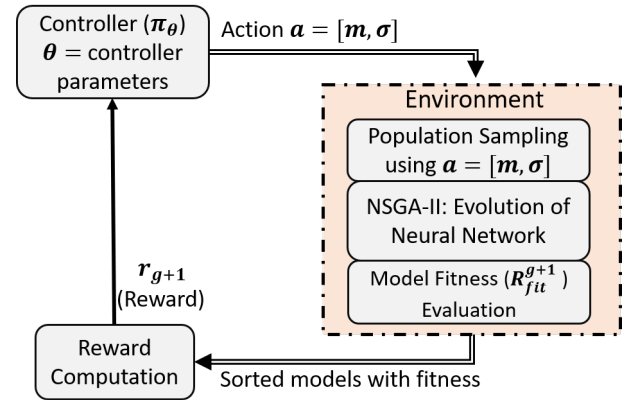


Fig. 2: Flow Diagram of guided sampling based NSGA-II.

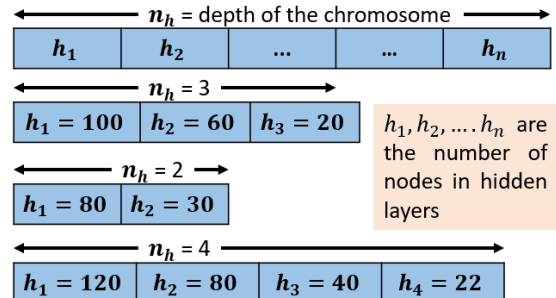


Fig. 3: Variable-length gene encoding strategy.

Algorithm 1 GS-EvoDNN: The Main Framework

Input: \mathcal{D}^{tr} & \mathcal{D}^{val} = training & validation datasets, n_R & h_R = Maximum depth & width of the DNN respectively
Output: Ψ^\dagger = best model after the termination or last generation of the evolution.

```

1:  $t \leftarrow 0$  //Set generation count ( $t$ ) = 0;
2:  $[m, \sigma] \leftarrow$  Compute mean and variance from allowable range for depth ( $n_R$ ) and width ( $h_R$ ) of the DNN.
3:  $P_0 \leftarrow \text{GuidedPop}(m, \sigma, N_p)$  //Generate  $N_p$  number of populations using Algorithm 2.
4:  $\Psi_0 \leftarrow$  Initialize weight matrices of the first model ( $P_0\{1\}$ ) by small random numbers.
5:  $\Lambda, \Psi_1^\dagger \leftarrow \text{FitnessEval}(P_0, \mathcal{D}^{tr}, \mathcal{D}^{val}, \Psi_0)$  //Evaluate fitness of all individuals in  $P_0$  using the Algorithm 3.
6:  $\mathcal{R} \leftarrow \text{NonDominatedSorting}(\Lambda_1)$  //Assign rank using non-dominated sorting [30].
7:  $P_1 \leftarrow \text{SelectParents}(P_0, \mathcal{R})$  //Select parents by binary tournament selection, [30].
8:  $\Lambda_s\{1\} \leftarrow \Lambda$  //Store the fitness History.
9:  $[m, \sigma] \leftarrow \text{UpdateMeanVar}(P_1, \Lambda_s)$  //Update mean and variance term using the Algorithm 4.
10:  $Q_1 \leftarrow \text{CrossoverMutation}(P_1, m, \sigma)$  //Apply crossover and mutation on  $P$  using Algorithm 5.
11:  $t \leftarrow t + 1$  //Update the generation count
12: while termination condition is false do
13:  $S_t \leftarrow (P_t \cup Q_t)$  //Combine the parent population ( $P_t$ ) & the child population ( $Q_t$ ).
14:  $\Lambda, \Psi_{t+1}^\dagger \leftarrow \text{FitnessEval}(S_t, \mathcal{D}^{tr}, \mathcal{D}^{val}, \Psi_t^\dagger)$  //Evaluate fitness of all individuals in  $S_t$  using the Algorithm 3.
15:  $\mathcal{R} \leftarrow \text{NonDominatedSorting}(\Lambda)$  //Assign rank by non-dominated sorting of fitness  $\Lambda$ , [30].
16:  $\mathcal{K} \leftarrow \text{CrowdingDistances}(S_t, \mathcal{R}, \Lambda)$  //Find crowding distances of individuals in population set  $S_t$ , [30].
17:  $P_{t+1} \leftarrow \text{SelectParentsByRankDist}(S_t, \mathcal{K}, \Lambda)$  //Select parents by crowding distance and rank, [30].
18:  $\Lambda_s\{t+1\} \leftarrow \Lambda$  //Store the fitness History.
19:  $[m, \sigma] \leftarrow \text{UpdateMeanVar}(S_t, \Lambda_s)$  //Update mean and variance term using the Algorithm 4.
20:  $Q_{t+1} \leftarrow \text{CrossoverMutation}(P_{t+1}, m, \sigma)$  //Apply crossover and mutation on  $P$  using Algorithm 5.
21: if Termination condition is true then
22:   Exit
23: else
24:    $t \leftarrow t + 1$  //Update the generation counter
25: end if
26: end while
27: Return: Best Model :  $\Psi^\dagger \leftarrow \Psi_{t+1}^\dagger$  //Best model of the last generation.
  
```

A. Population Sampling using Mean and Variance

AO includes depth and width variation in a defined search space. The real-coded gene encoding strategy is adopted to encode the depth as the number of genes (length of a chromosome) and the number of nodes in a hidden layer as the value of a gene as shown in Fig. 3. Let n_R & h_R be the maximum depth and width of the DNN, then the search space is defined as $[1 \ n_R]$ & $[1 \ h_R]$ for depth and the width variations. The mean and variance $m = [m_1, m_2]$ & $\sigma = [\sigma_1, \sigma_2]$ are initialized as $m_1 = (1 + n_R)/2$, $m_2 = (1 + h_R)/2$ and $\sigma_1 = (n_R - 1)/2$, $\sigma_2 = (h_R - 1)/2$.

Algorithm 2 GuidedPop: Population Sampling

Input: N = Population size, $m = [m_1, m_2]$ = mean & $\sigma = [\sigma_1, \sigma_2]$ = variance.
Output: P = Population with N chromosomes.

```

1:  $H \leftarrow$  generate  $N$  Gaussian numbers with  $m_1$  and  $\sigma_1$ .
2: for  $p = 1 : N$  do
3:  $h \leftarrow H(p)$  : depth of  $p^{th}$  chromosome
4:  $tmp \leftarrow$  generate  $h$  Gaussian numbers with  $m_2$  and  $\sigma_2$ .
5:  $P\{p\} \leftarrow$  convert all numbers in  $tmp$  to nearest integers.
6: end for
7: Return  $P$ 
  
```

B. Fitness Evaluation

Fast model evaluation is the most important requirement for NAS, especially when the evolutionary algorithm is used as an AO strategy. If the best model at a generation is transferred for initialization of the DNN weight matrices in the next generation, it makes the training and evaluation of the models faster. The quick learning mechanism suggested in [16] is adopted for the fitness evaluation as shown in Fig. 4. For the first generation, DNN models are initialized randomly and trained using Limited-Broyden-Fletcher-Goldfarb-Shanno (LBFGS) [51] algorithm. For next-generation and onward, the best model obtained is transformed (Fig. 4) to initialize the models followed by fine-tuning with the LBFGS algorithm for a few iterations only. If a model Ψ^t at generation t^{th} has weight matrix W^t , the classification loss \mathcal{J} for a C problem can be defined in term of $[w, b] \in W^t$ as

$$\mathcal{J}(W^t) = \frac{1}{n^s} \left[\sum_{k=1}^{n^s} \sum_{i=1}^C I[y_k = c_i] \log \frac{e^{(w_i^T f(x_p) + b_i)}}{\sum_{i=1}^C e^{(w_i^T f(x_p) + b_i)}} \right] \quad (7)$$

where, $f(x) = \Phi(wx + b)$ is the h-level features representation of DNN, y_k be the output label of the k^{th} data sample and c_i denotes the i^{th} class. The classification accuracy (CA) of fine-tuned model for the validation data is returned as the fitness

of that model.

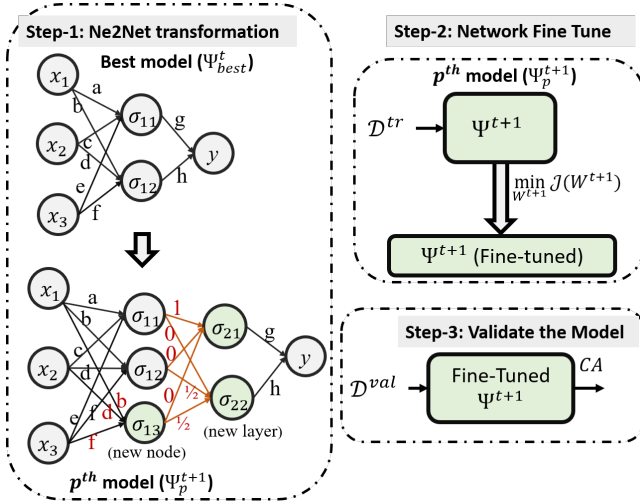


Fig. 4: Fitness evaluation strategy.

Algorithm 3 FitnessEval: Fitness Evaluation

Input: P = Population with population size N_p ,
 $(\mathcal{D}^{tr}, \mathcal{D}^{val})$ = Training & validation data.

Output: Λ = Fitness matrix and Ψ^\dagger = Best model.

- 1: $t \leftarrow$ current generation
 - 2: **for** $p = 1 : N_p$ **do**
 - 3: $\Psi_t \leftarrow$ N2N(Ψ_t^\dagger) // Transform Ψ_t^\dagger as p^{th} model using N2N transformation as depicted in step-1 of Fig. 4.
 - 4: Fine-tune the model (Ψ_t) on \mathcal{D}^{tr} to minimize Eq. (7).
 - 5: $\Lambda(p) \leftarrow$ Find CA of Ψ_t on dataset \mathcal{D}^{val} .
 - 6: **end for**
 - 7: $\Psi_t^\dagger \leftarrow$ Best model // Find the model with maximum CA and minimum number of model parameters.
 - 8: Return Λ, Ψ_t^\dagger
-

C. Update Mean and Variance using PG

Mean (m) and variance (σ) terms are used for sampling of a new population as illustrated in Section-IV-A. Here, we design a PG-based update laws for m & σ such that the best fitness ($\max(\Lambda)$) is maximized. At any generation t , $\max(\Lambda)$ is termed as reward, $a_t = [m, \sigma]$ is termed as action, and weighted average of fitness (Λ) is termed as state of the policy. Thus, the policy generates $[m^T, \sigma^T]$ to guide the evolution for faster and better convergence. For the design simplification, let us assume that the action is generated by a deterministic policy as

$$a_t = f(\theta_t) = \frac{1}{1 + e^{-\theta_t}} \quad (8)$$

where, policy parameter θ_t is selected such that it controls $m \in \mathbb{R}^2$ (mean of depth and width of DNN) and $\sigma \in \mathbb{R}^2$ (variance for depth and width of DNN). The parameter θ is updated by the policy gradient in (3) calculated using gradient of expected total reward U_t derived in (6). The total cumulative reward is calculated using fitness matrix Λ_t at generation t as

in (9).

$$U_t = \sum_{i=1}^t \frac{\max(\Lambda_i) - \max(\Lambda_{i-1})}{\max(\Lambda_{i-1})} \quad (9)$$

The algorithmic steps for the implementation of policy gradient based update of $a_t = [m, \sigma]$ at generation t is summarised in Algorithm 4.

Algorithm 4 UpdateMeanVar: Update m & σ using PG

Input: P_t = Current population, Λ = Fitness matrix,
 $a_{t-1} = [m, \sigma]$ = Initial mean & variance term.

Output: $a_t = [m, \sigma]$ = Updated mean & variance.

- 1: N = Number of models in P_t , α = Learning rate
 - 2: $\bar{n} \leftarrow$ Compute average depth of models in P_t
 - 3: $\Omega = [\omega_p]_{p=1}^N$ //Generate a set of weights ω_p such that $\sum_{p=1}^N \omega_p = 0$ and $\omega_1 > \omega_2 > \dots > \omega_N$
 - 4: $\Lambda_t^{sorted}, idx = \text{sort}(\Lambda_t, \text{'descending'})$
 - 5: $P_t \leftarrow$ Sort P_t according to idx .
 - 6: n_p = no. of hidden layers (depth) in p^{th} model.
 - 7: $\delta_p = \max(H_p) - \min(H_p)$ // H_p = set of nodes in hidden layers of p^{th} model
 - 8: **if** $t \leq 1$ **then**
 - 9: $m = \sum_{j=1}^N \left[n_p \omega_p \quad \frac{1}{n_p} \sum_{k=1}^{n_p} h_{kp} \omega_p \right]$ // $h_{kp} \in H_p$.
 - 10: $\sigma = \sum_{j=1}^N [(\bar{n} - n_p) \omega_p \quad \delta_p \omega_p / 2]$
 - 11: **else**
 - 12: $\theta_{t-1} = \ln [a_{t-1} / (1 - a_{t-1})]$
 - 13: $U_t \leftarrow$ Compute cumulative reward using (9).
 - 14: $s_m = \sum_{j=1}^N \left[n_p \omega_p \quad \frac{1}{n_p} \sum_{k=1}^{n_p} h_{kp} \omega_p \right]$
 - 15: $s_\sigma = \sum_{j=1}^N [(\bar{n} - n_p) \omega_p \quad \delta_p \omega_p / 2]$
 - 16: $s_t = [s_m^T \quad s_\sigma^T]$
 - 17: $\theta_t \leftarrow \theta_{t-1} + \alpha * \frac{1}{N} \sum_{k=1}^N U_t E[\nabla \log \pi_\theta(s_t | a_{t-1}; \theta)]$
 - 18: $a_t = 1 / (1 + e^{-\theta_t})$
 - 19: **end if**
 - 20: Return a_t
-

D. Crossover and Mutation

For the optimal search of the network architecture, a combination of exploration and exploitation strategies is adopted. The guided sampling-based generation of new population exploits the search space to force the evolution towards maximum accuracy. To avoid local convergence, N number of individuals are sampled using m and σ based on Gaussian distribution, and also N number of parent populations are selected using crowding distance and rank from the current generation. After that, the two populations are merged to create a double-sized mating pool. Now, the two-step crossover operator introduced in [26] is applied. The two steps are (i) single point depth crossover (SPDC) for depth variation and (ii) common depth simulated binary crossover (CDSBC) for gene value (width) alteration. The two-step crossover method is depicted in Fig. 5. The whole process of offspring generation is provided in Algorithm 5:

V. EXPERIMENTAL RESULTS AND DISCUSSION

The efficacy of the proposed framework of GS-EvoDNN is demonstrated on fault diagnosis dataset under different

n_1, n_2 = model depth, h_{11}, h_{12}, \dots = no. of nodes in hidden layers

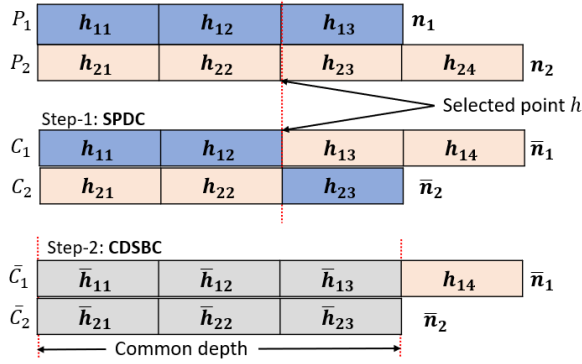


Fig. 5: Two-steps crossover for chromosomes with different length.

Algorithm 5 Offspring Generation: Crossover and Mutation

Input: P = Parent population, p_c = Crossover probability, (m, σ) = mean & variance term for sampling.

Output: Q = Offspring population.

- 1: $Q \leftarrow \text{GuidedPop}(m, \sigma, N, n_R, h_R)$ //Generate N offspring populations using Algorithm 2.
- 2: I_c = generate random indices of $p_c * 100\%$ members from P .
- 3: **for** $i \in I_c$ **do**
- 4: Select $P_1 = P\{i\}$ & $P_2 = Q\{i\}$.
- 5: Find lengths (n_1, n_2) of P_1, P_2
- 6: Set a point $h < \min(n_1, n_2)$ on P_1, P_2 .
- 7: $C_1, C_2 \leftarrow \text{SPDC}$ of P_1, P_2 at point h (as depicted in **step-1 of Fig. 5**)
- 8: $\bar{C}_1, \bar{C}_2 \leftarrow \text{CDSBC}$ for genes of the common depth portion of C_1, C_2 as depicted in **step-2 of Fig. 5**.
- 9: Replace $Q\{i\}$ by \bar{C}_1 or \bar{C}_2 .
- 10: **end for**
- 11: Return Q

operating conditions taken from (i) Air compressor fault data [52], (ii) Paderborn University (PBU) bearing fault data [53], and (iii) CWRU bearing fault data [54].

A. Experimental Setup

1) *Air Compressor Fault Data* [52]: The air compressor data contains acoustic signal recorded on single stage reciprocating type air compressor driven by an 5hp induction motor installed at the workshop, EE Department, IIT Kanpur. Data were recorded in eight different cases: healthy and seven different faulty states of the air compressor valve. Therefore, the dataset has 8 classes: (i) Healthy (**H**), (ii) Leakage Inlet Valve (**LIV**), (iii) Leakage Outlet Valve (**LOV**), (iv) Non-Return Valve (**NRV**), (v) Piston Ring (**PR**), (vi) Flywheel (**F**), (vii) Rider Belt (**RB**), and (viii) Bearing (**B**). For each class, 225 measurements were taken with 50k samples in each measurement.

2) *PBU Bearing Fault Data* [53]: PBU bearing fault data is the collection of time-series signals recorded on electrical machine operating under wide variation of shaft load and rotational speed. The four Load and speed settings (LS) are

LS1: N09_M07_F10 (speed = 900 rpm, torque = 0.7 Nm & radial force = 1000 N), **LS2: N15_M01_F10** (speed = 1500 rpm, torque = 0.1 Nm & radial force = 1000 N), **LS3: N15_M07_F04** (speed = 1500 rpm, torque = 0.7 Nm & radial force = 400 N), and **LS4: N15_M07_F10** (speed = 1500 rpm, torque = 0.7 Nm & radial force = 1000 N). Total of 32 experimentation with 6 healthy, 12 artificially damaged, and 14 damaged by long run accelerated tests were conducted to record current, vibration signal, radial forces, torque, and bearing temperature. The recorded signals contains two types of faults: inner race (**IR**) fault and outer race (**OR**) fault.

3) *CWRU Bearing Fault Data* [54]: The CWRU bearing fault data provided by Case Western Reserve University (CWRU) has been a widely used benchmark dataset for bearing fault diagnosis. It contains vibration signal recorded at drive-end (DE) and fan-end (FE) of bearing artificially seeded with inner race fault (**IR**), outer race (**OR**), and rolling element ball (**B**) faults of variable fault diameters (F.D.) (from 0.007 to 0.028 inches). The bearing test rig setup details can be found in [54].

B. Segmentation and Data Processing

The recorded time-series signals contain a huge number of samples which is not suitable for training the DNN. To make the dimension of the time-series signals compatible with the DNN, we adopt a segmentation rule with the segment length of approximately $1/4^{th}$ of data points recorded per revolution. Here, we have selected segmentation lengths of 100, 200, & 400 for the CWRU dataset, Air compressor dataset, and PBU dataset respectively. Also, the time-series signals are usually unstructured and not to the scale. Therefore, we have applied the min-max normalization technique to scale down the dataset to $[0, 1]$. The min-max normalization also removes the effect of outlier points. If for some cases, the outlier points carry some important information, then the z-score minimization technique may be used to make the dataset well-structured [16].

C. Dataset Preparation

For the study of fault diagnosis with the proposed GS-EvoDNN, we prepare the training, the validation, & the testing dataset under various operating conditions described below.

Case-1 (T1): From *Air Compressor Dataset*, 7 different cases of binary classes and one case of multi-class diagnosis are investigated as listed in table II. For each class, 4 measurement files (having 50k samples/file) are merged to create a sample of size 1000×200 per class taking 200 points as segment length.

Case-2 (T2): From *CWRU FE Dataset*, multi-class diagnosis with class name healthy (**H**), inner race (**IR**), outer race (**OR**), and ball element (**B**) are considered under different load (1, 2, & 3 hp) conditions and different fault diameters (FD) (7, 14, & 21 mil). For each FD (for example, 7 mil), dataset from all three load conditions are prepared. Thus, the fault diagnosis on total of 9 cases are presented as listed in table III.

Table II: AIR COMPRESSOR DATASET (T1): DIAGNOSTIC PERFORMANCE IN TERM OF CLASSIFICATION ACCURACY

Class	SVM [35]	DNN [7]	DTL [13]	DAFD [12]	N2N [16]		EvoDCNN [25]	EvoN2N [26]	GS-EvoDNN
					W. D. A.	D. A.			
H-LIV	99.75	96.25	99.00	99.75	99.50	99.75	100.00	100.00	100.00
H-LOV	98.25	95.75	99.25	99.66	99.25	99.25	99.75	99.75	100.00
H-PR	98.25	93.25	93.30	98.75	97.75	98.75	98.25	99.75	99.75
H-B	98.25	98.50	98.75	98.75	96.75	98.75	98.75	99.75	100.00
H-F	99.25	99.25	99.00	98.75	99.25	99.25	99.25	100.00	100.00
H-NRV	98.75	99.00	99.00	99.75	99.00	99.25	99.25	100.00	100.00
H-RB	98.25	98.25	98.25	99.00	99.75	99.75	99.25	100.00	100.00
H-ALL	97.75	99.25	99.00	99.00	99.25	99.25	99.75	99.75	100.00
S. D.	0.65	2.16	2.00	0.46	1.02	0.38	0.57	0.13	0.09

Table III: CWRU FE DATASET (T2): DIAGNOSTIC PERFORMANCE IN TERM OF CLASSIFICATION ACCURACY

Class	F.D.	Load	SVM [35]	DNN [7]	DTL [13]	DAFD [12]	N2N [16]		EvoDCNN [25]	EvoN2N [26]	GS-EvoDNN
							W. D. A.	D. A.			
H-IR-OR-B	DE 7 mil	1hp	88.12	96.69	96.56	97.94	98.94	98.94	99.60	100.00	100.00
		2hp	98.12	95.94	93.44	96.12	97.12	98.12	99.60	100.00	100.00
		3hp	99.10	98.75	98.75	98.44	99.44	99.44	99.70	100.00	100.00
	DE 14 mil	1hp	99.10	94.75	96.88	97.19	99.19	99.67	100.00	100.00	100.00
		2hp	98.10	95.31	92.19	95.69	97.69	98.69	98.12	99.12	99.60
		3hp	99.25	96.88	94.69	97.62	99.33	98.62	98.44	98.84	100.00
	DE 21 mil	1hp	96.88	86.56	84.69	89.62	95.62	96.62	93.75	98.75	100.00
		2hp	88.44	85.31	82.19	86.69	90.69	90.69	90.10	95.37	98.85
		3hp	92.19	86.56	79.38	88.06	91.06	92.06	92.81	95.81	98.81
	S. D.		4.62	5.25	7.06	4.66	3.46	3.32	3.69	1.81	0.51

Table IV: CA FOR TARGET-2 & TARGET-3 DATASET AND FOR VERY LIMITED SAMPLES OF TARGET-2 & TARGET-3 DATASET

Class	Data-L.S.	SVM [35]	DNN [7]	DTL [13]	DAFD [12]	N2N [16]		EvoDCNN [25]	EvoN2N [26]	GS-EvoDNN
						W. D. A.	D. A.			
H-OR-IR	T3-L1	94.25	96.92	96.92	96.92	98.64	98.94	99.25	99.75	100.00
	T3-L2	90.00	93.58	95.00	94.58	95.12	96.12	99.58	99.83	99.75
	T3-L3	87.17	91.92	93.33	92.08	94.44	94.44	97.50	97.70	100.00
	T3-L4	87.17	93.15	93.75	94.17	97.19	95.28	100.00	100.00	100.00
	T4-L1	95.00	97.50	97.50	98.33	98.33	99.17	99.17	100.00	100.00
	T4-L2	92.83	95.92	96.50	96.33	96.33	96.33	98.60	99.15	100.00
	T4-L3	94.83	94.67	93.33	94.17	95.72	96.33	98.60	99.15	100.00
	T4-L4	94.83	95.33	95.00	95.83	95.69	95.69	93.33	98.75	99.75
S. D.		3.41	1.92	1.65	1.95	1.50	1.68	2.13	0.79	0.10

Case-3 (T3 & T4): From *PBU Dataset*, two different cases are considered (i) T3: artificially damaged bearing fault and (ii) T4: bearing fault due to long accelerated test. In both cases, multi-class diagnosis with three classes namely **H-OR-IR** is studied under four load settings (LS) as listed in table IV.

Now for the training, the validation, & the testing, each of the above dataset is split into three portions: 64% train (\mathcal{D}^{tr}), 20% test (\mathcal{D}^{te}), and 16% validate (\mathcal{D}^{val}) datasets.

D. Implementation Details

For the implementation of the proposed framework of GS-EvoDNN, the initial parameters are selected as: population size (N) = 100, crossover probability (P_c) = 0.5, and the maximum number of generations is set to very high usually at 50. Also, the termination criteria are set as either the validation accuracy reaches 100% or it does not change continuously for 3 generations. The allowable ranges for the variation of depth and width are selected as $n_R \in [1, 10]$ and $h_R \in [10, 400]$ respectively. The learning rate $\alpha = 0.1$. The GS-EvoDNN framework is applied to the training dataset and the best model obtained is tested for the test dataset under all cases (T1,

T2, T3, & T4) described in section V-C. The classification accuracies (CA) are tabulated in tables II, III, & IV.

For comparison and analysis, the state-of-the-art methods for intelligent fault diagnosis best reported in various literature are selected as support vector machines (SVM) [35], deep neural network (DNN) [7], deep transfer learning (DTL) based on sparse autoencoder [13], Deep neural network for domain Adaptation in Fault Diagnosis (DAFD) [12], Net2Net without domain adaptation (N2N_WDA) [16], Net2Net with domain adaptation (N2N_DA) [16], evolutionary deep CNN (EvoDCNN) [25], and evolutionary Net2Net (EvoN2N) [26]. The DNN, DTL, and DAFD are trained with hidden sizes as (70–50–20). The initial and hyper parameters for EvoDCNN and EvoN2N are kept same as mentioned above. The same dataset (T1, T2, T3, & T4) are used to train and test all these methods using the procedure suggested in the corresponding cited references. The diagnostic performance in term of CA are tabulated in tables II, III, & IV. The standard deviation (S.D.) of CA calculated over the variation in the operating conditions is also tabulated to compare the result deviation with the change in the operating conditions.

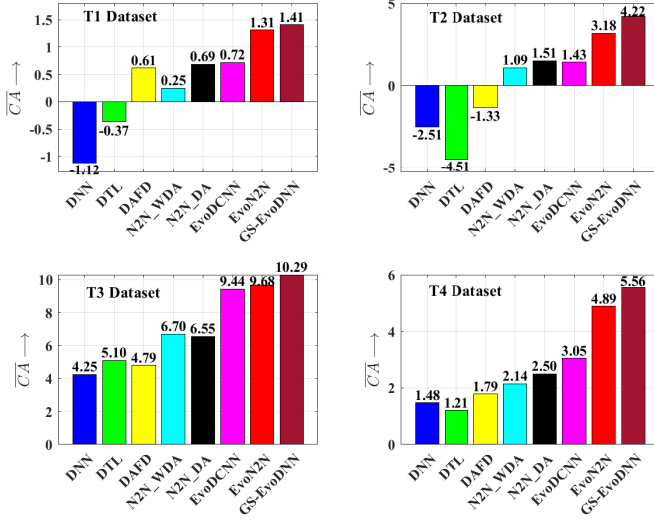


Fig. 6: TI in term of \overline{CA} for (i) T1: Air Compressor dataset, (ii) T2: CWRU dataset, (iii) T3: PBU dataset with single point fault, and (iv) T4: PBU dataset with distributed fault.

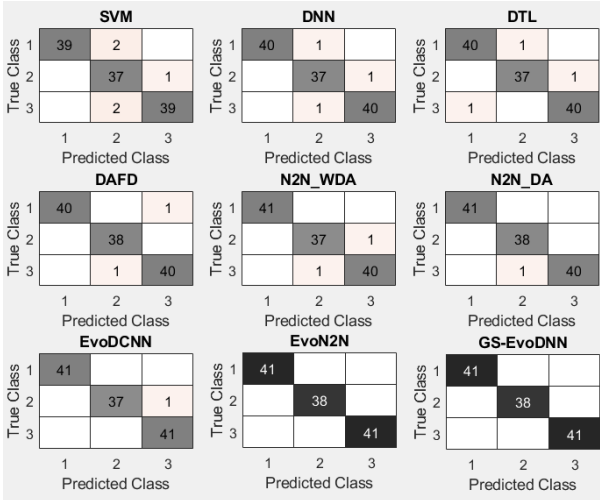


Fig. 7: Confusion matrix for dataset T4-L1 (Table IV): class label {'1', '2', '3'} represents the class name {'H', 'OR', 'IR'}.

E. Discussion

The diagnostic performances by the proposed method and the selected state-of-the-art methods conclude the following important points.

- 1) The CA comparison in tables II, III, & IV reveal that the diagnostic performances are very much affected by the model selection. The DNN model with the best suitable architecture for the given dataset gives CA up to almost 100% whereas other methods with pre-selected architecture fail to perform well.
- 2) Considering SVM [35] as the baseline diagnostic method, We evaluate the transfer improvement (TI) in term of average CA for the dataset T1, T2, T3, & T4 separately. If the average CA is denoted as \overline{CA} , the TI is defined as $TI = \overline{CA} - \overline{CA}_b$, where \overline{CA}_b is the average CA by SVM. The TI graph shown in Fig. 6 shows the performance improvement of the proposed framework in comparison with the state-of-the-art methods and the

baseline method 'SVM'.

- 3) The performance comparison between EvoN2N [26] and the proposed method shows that architecture optimization is greatly affected by the guided sampling with policy gradient framework.
- 4) Fig. 7 demonstrate the classification performance by confusion chart matrices for one of the dataset (T4-L1: table IV). Classifications with 100% accuracies are highlighted by blackened diagonal elements where for other cases, diagonal elements are highlighted by gray shade.
- 5) The comparison between EvoDCNN [25], EvoN2N [26], & the proposed GS-EvoN2N reveal that the DNN model with the best architecture performs better than the CNN model for fault diagnosis applications with the segmented dataset (described in section V-B).

F. Complexity Analysis

The worst complexities in one iteration of the entire algorithm 1 are contributed by (i) fitness evaluation of the DNN model and (ii) the non-dominated sorting. The complexity of the fitness evaluation of DNN is mainly contributed by parameter optimization by L-BFGS which is $O(N_I * n^2)$, where n & N_I be the total number of parameters and number of iterations required to fine-tune the DNN model. The non-dominated sorting algorithm has a complexity of $O(MN_p^2)$, where M & N_p^2 be the number of objectives and the population size respectively. Since M is very small compared to N_I , therefore, the time complexity for GS-EvoDNN with population size N_p is given by $O(N_I N_p n^2)$, where n = total number of parameters in one model and N_I = number of iterations taken for model training.

VI. CONCLUSIONS

In this article, we have formulated a guided sampling-based evolutionary algorithm for DNN architecture search. The proposed framework uses the concept of policy gradient to sample the new population to force the evolution towards the maximization of classification performance. The best model obtained at any generation is transferred to the next generation to initialize the model evaluation which makes the entire algorithm faster. Therefore, this method is very good in terms of faster evolution and faster convergence while ensuring global convergence by update policy of mean and variance. The validation using dataset under various cases from Air Compressor data, CWRU data, and PBU data prove that the proposed framework is capable to obtain the best model to get diagnostic performance almost up to 100% accuracy. This method can also be employed for the architecture optimization of the CNN model with image classification applications.

REFERENCES

- [1] S. Nandi, H. A. Toliyat, and X. Li, "Condition monitoring and fault diagnosis of electrical motors—a review," *IEEE Transactions on Energy Conversion*, vol. 20, no. 4, pp. 719–729, Dec 2005.
- [2] A. Siddique, G. S. Yadava, and B. Singh, "A review of stator fault monitoring techniques of induction motors," *IEEE Transactions on Energy Conversion*, vol. 20, no. 1, pp. 106–114, March 2005.

- [3] S. Yin, S. X. Ding, X. Xie, and H. Luo, "A review on basic data-driven approaches for industrial process monitoring," *IEEE Transactions on Industrial Electronics*, vol. 61, no. 11, pp. 6418–6428, 2014.
- [4] X. Chen, S. Wang, B. Qiao, and Q. Chen, "Basic research on machinery fault diagnostics: Past, present, and future trends," *Front. Mech. Eng.*, vol. 13, p. 264–291, 2018.
- [5] Z. Chen, F. Han, L. Wu, J. Yu, S. Cheng, P. Lin, and H. Chen, "Random forest based intelligent fault diagnosis for pv arrays using array voltage and string currents," *Energy conversion and management*, vol. 178, pp. 250–264, 2018.
- [6] A. K. Sharma, V. Singh, N. K. Verma, and J. Liu, "Condition based monitoring of machine using mamdani fuzzy network," in *2018 Prognostics and System Health Management Conference (PHM-Chongqing)*, Oct 2018, pp. 1159–1163.
- [7] Y. Qi, C. Shen, D. Wang, J. Shi, X. Jiang, and Z. Zhu, "Stacked sparse autoencoder-based deep network for fault diagnosis of rotating machinery," *IEEE Access*, vol. 5, pp. 15 066–15 079, 2017.
- [8] R. Zhao, R. Yan, Z. Chen, K. Mao, P. Wang, and R. X. Gao, "Deep learning and its applications to machine health monitoring," *Mechanical Systems and Signal Processing*, vol. 115, pp. 213 – 237, 2019.
- [9] S. J. Pan, I. W. Tsang, J. T. Kwok, and Q. Yang, "Domain adaptation via transfer component analysis," *IEEE Transactions on Neural Networks*, vol. 22, no. 2, pp. 199–210, Feb 2011.
- [10] M. Long, J. Wang, G. Ding, S. J. Pan, and P. S. Yu, "Adaptation regularization: A general framework for transfer learning," *IEEE Transactions on Knowledge and Data Engineering*, vol. 26, no. 5, pp. 1076–1089, 2014.
- [11] Y. Ganin, E. Ustinova, H. Ajakan, P. Germain, H. Larochelle, F. Laviolette, M. March, and V. Lempitsky, "Domain-adversarial training of neural networks," *Journal of Machine Learning Research*, vol. 17, no. 59, pp. 1–35, 2016.
- [12] W. Lu, B. Liang, Y. Cheng, D. Meng, J. Yang, and T. Zhang, "Deep model based domain adaptation for fault diagnosis," *IEEE Transactions on Industrial Electronics*, vol. 64, no. 3, pp. 2296–2305, March 2017.
- [13] L. Wen, L. Gao, and X. Li, "A new deep transfer learning based on sparse auto-encoder for fault diagnosis," *IEEE Transactions on Systems, Man, and Cybernetics: Systems*, vol. 49, no. 1, pp. 136–144, Jan 2019.
- [14] L. Guo, Y. Lei, S. Xing, T. Yan, and N. Li, "Deep convolutional transfer learning network: A new method for intelligent fault diagnosis of machines with unlabeled data," *IEEE Transactions on Industrial Electronics*, vol. 66, no. 9, pp. 7316–7325, Sep. 2019.
- [15] D. Wei, T. Han, F. Chu, and M. J. Zuo, "Weighted domain adaptation networks for machinery fault diagnosis," *Mechanical Systems and Signal Processing*, vol. 158, p. 107744, 2021.
- [16] A. K. Sharma and N. K. Verma, "Quick learning mechanism with cross-domain adaptation for intelligent fault diagnosis," 2021.
- [17] G. Wang, J. Qiao, J. Bi, W. Li, and M. Zhou, "Tl-gdbn: Growing deep belief network with transfer learning," *IEEE Transactions on Automation Science and Engineering*, vol. 16, no. 2, pp. 874–885, April 2019.
- [18] X. He, K. Zhao, and X. Chu, "Automl: A survey of the state-of-the-art," *Knowledge-Based Systems*, vol. 212, p. 106622, 2021.
- [19] J. Bergstra and Y. Bengio, "Random search for hyper-parameter optimization," *J. Mach. Learn. Res.*, vol. 13, pp. 281–305, Feb. 2012.
- [20] F. Hutter, H. H. Hoos, and K. Leyton-Brown, "Sequential model-based optimization for general algorithm configuration," in *Learning and Intelligent Optimization*, C. A. C. Coello, Ed. Berlin, Heidelberg: Springer Berlin Heidelberg, 2011, pp. 507–523.
- [21] B. Baker, O. Gupta, N. Naik, and R. Raskar, "Designing neural network architectures using reinforcement learning," *CoRR*, vol. abs/1611.02167, 2016.
- [22] S. M. R. Loghmanian, H. Jamaluddin, R. Ahmad, R. Yusof, and M. Khalid, "Structure optimization of neural network for dynamic system modeling using multi-objective genetic algorithm," *Neural Computing and Applications*, vol. 21, no. 6, pp. 1281–1295, 2012.
- [23] C. Wang, C. Xu, X. Yao, and D. Tao, "Evolutionary generative adversarial networks," *IEEE Transactions on Evolutionary Computation*, vol. 23, no. 6, pp. 921–934, 2019.
- [24] Y. Sun, B. Xue, M. Zhang, and G. G. Yen, "A particle swarm optimization-based flexible convolutional autoencoder for image classification," *IEEE Transactions on Neural Networks and Learning Systems*, vol. 30, no. 8, pp. 2295–2309, Aug 2019.
- [25] Y. Sun, B. Xue, M. Zhang, and G. G. Yen, "Evolving deep convolutional neural networks for image classification," *IEEE Transactions on Evolutionary Computation*, vol. 24, no. 2, pp. 394–407, 2020.
- [26] A. K. Sharma and N. K. Verma, "Transfer learning based evolutionary deep neural network for intelligent fault diagnosis," 2021.
- [27] H. Liu, K. Simonyan, and Y. Yang, "Darts: Differentiable architecture search," in *International Conference on Learning Representations*, 2019.
- [28] Z. Yang, Y. Wang, X. Chen, B. Shi, C. Xu, C. Xu, Q. Tian, and C. Xu, "Cars: Continuous evolution for efficient neural architecture search," in *Proceedings of the IEEE/CVF Conference on Computer Vision and Pattern Recognition*, 2020, pp. 1829–1838.
- [29] E. Real, A. Aggarwal, Y. Huang, and Q. V. Le, "Regularized evolution for image classifier architecture search," *Proceedings of the AAAI Conference on Artificial Intelligence*, vol. 33, no. 01, pp. 4780–4789, Jul. 2019. [Online]. Available: <https://ojs.aaai.org/index.php/AAAI/article/view/4405>
- [30] K. Deb, A. Pratap, S. Agarwal, and T. Meyarivan, "A fast and elitist multiobjective genetic algorithm: NSGA-II," *IEEE Transactions on Evolutionary Computation*, vol. 6, no. 2, pp. 182–197, 2002.
- [31] Z. Lu, I. Whalen, Y. Dhebar, K. Deb, E. D. Goodman, W. Banzhaf, and V. N. Boddeti, "Multiobjective evolutionary design of deep convolutional neural networks for image classification," *IEEE Transactions on Evolutionary Computation*, vol. 25, no. 2, pp. 277–291, 2021.
- [32] G. E. Hinton and R. R. Salakhutdinov, "Reducing the dimensionality of data with neural networks," *Science*, vol. 313, no. 5786, pp. 504–507, 2006.
- [33] Y. Bengio, P. Lamblin, D. Popovici, and H. Larochelle, "Greedy layer-wise training of deep networks," in *Advances in Neural Information Processing Systems 19*, B. Schölkopf, J. C. Platt, and T. Hoffman, Eds. MIT Press, 2007, pp. 153–160.
- [34] H. Su and K. T. Chong, "Induction machine condition monitoring using neural network modeling," *IEEE Transactions on Industrial Electronics*, vol. 54, no. 1, pp. 241–249, 2007.
- [35] A. Widodo and B.-S. Yang, "Support vector machine in machine condition monitoring and fault diagnosis," *Mechanical Systems and Signal Processing*, vol. 21, no. 6, pp. 2560–2574, 2007.
- [36] X. Yan and M. Jia, "A novel optimized svm classification algorithm with multi-domain feature and its application to fault diagnosis of rolling bearing," *Neurocomputing*, vol. 313, pp. 47–64, 2018.
- [37] S. D. Juan Jose, *et al.*, "Multifault diagnosis method applied to an electric machine based on high-dimensional feature reduction," *IEEE Transactions on Industry Applications*, vol. 53, no. 3, pp. 3086–3097, 2016.
- [38] X. Li, W. Zhang, and Q. Ding, "Cross-domain fault diagnosis of rolling element bearings using deep generative neural networks," *IEEE Transactions on Industrial Electronics*, vol. 66, no. 7, pp. 5525–5534, July 2019.
- [39] B. Zoph, V. Vasudevan, J. Shlens, and Q. V. Le, "Learning transferable architectures for scalable image recognition," in *Proc. IEEE Comput. Soc. Conf. Comput. Vis. Pattern Recognit.*, 2018, pp. 8697–8710.
- [40] A. Hundt, V. Jain, and G. D. Hager, "sharpdarts: Faster and more accurate differentiable architecture search," *CoRR*, vol. abs/1903.09900, 2019. [Online]. Available: <http://arxiv.org/abs/1903.09900>
- [41] K. Kandasamy, W. Neiswanger, J. Schneider, B. Póczos, and E. P. Xing, "Neural architecture search with bayesian optimisation and optimal transport," in *Proceedings of the 32nd International Conference on Neural Information Processing Systems*, ser. NIPS'18, 2018, p. 2020–2029.
- [42] J. S. Bergstra, R. Bardenet, Y. Bengio, and B. Kégl, "Algorithms for hyper-parameter optimization," in *Advances in Neural Information Processing Systems 24*, J. Shawe-Taylor, R. S. Zemel, P. L. Bartlett, F. Pereira, and K. Q. Weinberger, Eds. Curran Associates, Inc., 2011, pp. 2546–2554.
- [43] H. Pham, M. Guan, B. Zoph, Q. Le, and J. Dean, "Efficient neural architecture search via parameters sharing," in *International Conference on Machine Learning*. PMLR, 2018, pp. 4095–4104.
- [44] R. Luo, F. Tian, T. Qin, E. Chen, and T.-Y. Liu, "Neural architecture optimization," in *Advances in Neural Information Processing Systems*, S. Bengio, H. Wallach, H. Larochelle, K. Grauman, N. Cesa-Bianchi, and R. Garnett, Eds., vol. 31. Curran Associates, Inc., 2018.
- [45] B. Zoph and Q. V. Le, "Neural architecture search with reinforcement learning," *arXiv preprint arXiv:1611.01578*, 2016.
- [46] J. Sun, X. Liu, T. Bäck, and Z. Xu, "Learning adaptive differential evolution algorithm from optimization experiences by policy gradient," *IEEE Transactions on Evolutionary Computation*, vol. 25, no. 4, pp. 666–680, 2021.
- [47] Y. Chen, G. Meng, Q. Zhang, S. Xiang, C. Huang, L. Mu, and X. Wang, "Renas: Reinforced evolutionary neural architecture search," in *Proceedings of the IEEE/CVF Conference on Computer Vision and Pattern Recognition*, 2019, pp. 4787–4796.
- [48] Y. Sun, H. Wang, B. Xue, Y. Jin, G. G. Yen, and M. Zhang, "Surrogate-assisted evolutionary deep learning using an end-to-end random forest-

- based performance predictor,” *IEEE Transactions on Evolutionary Computation*, vol. 24, no. 2, pp. 350–364, 2019.
- [49] R. J. Williams, “Simple statistical gradient-following algorithms for connectionist reinforcement learning,” *Machine Learning*, vol. 8, no. 3-4, p. 229–256, May 1992.
 - [50] R. Sutton and A. Barto, *Reinforcement Learning: An Introduction, second edition*, ser. Adaptive Computation and Machine Learning series. MIT Press, 2018.
 - [51] J. Nocedal and S. J. Wright, *Large-Scale Unconstrained Optimization*. New York, NY: Springer New York, 2006, pp. 164–192.
 - [52] N. K. Verma, R. K. Sevakula, S. Dixit, and A. Salour, “Intelligent condition based monitoring using acoustic signals for air compressors,” *IEEE Transactions on Reliability*, vol. 65, no. 1, pp. 291–309, March 2016.
 - [53] C. Lessmeier, J. Kimotho, D. Zimmer, and W. Sextro, “Condition monitoring of bearing damage in electromechanical drive systems by using motor current signals of electric motors: A benchmark data set for data-driven classification,” *European Conf., PHM Society, Bilbao (Spain)*, vol. 3, no. 1, 2016.
 - [54] W. A. Smith and R. B. Randall, “Rolling element bearing diagnostics using the Case Western Reserve University data: A benchmark study,” *Mechanical Systems and Signal Processing*, vol. 64, pp. 100–131, 2015.